6240 *Chem. Mater.* **2010,** *22,* 6240–6245
DOI:10.1021/cm101609p

CHEMISTRY OF MATERIALS
Article

Encapsulation of Phosphine-Terminated Rhenium(III) Chalcogenide Clusters in Silica Nanoparticles

Lei Gao, Miya A. Peay, and Thomas G. Gray*

Department of Chemistry, Case Western Reserve University, 10900 Euclid Avenue, Cleveland, Ohio 44106, United States

Received June 9, 2010. Revised Manuscript Received October 20, 2010

Cationic phosphine-terminated rhenium(III) chalcogenide clusters—$[Re_6Se_8(Et_3P)_5I]I$, $[Re_6S_8(Et_3P)_5Br]Br$, $[Re_6Se_8(Bu_3P)_5I]I$, and $[Re_6S_8(Bu_3P)_5Br]Br$—were synthesized and encapsulated in silica nanospheres in a one-pot, base-catalyzed hydrolysis in acetonitrile. The cluster-doped silica nanoparticles have diameters of 10−20 nm, as observed by transmission electron microscopy (TEM). The diameter is dependent upon the volume of the solvent added to the system. Reactions conducted in >10 mL of acetonitrile led to the isolation of particles ~200 nm in diameter. The absorption and emission properties of the clusters were maintained upon encapsulation. The ^1H resonance of the alkyl groups was not observed in the silica-cluster composites via nuclear magnetic resonance (NMR), and the emission blue-shifts, indicating that the clusters reside within the silica framework, rather than on the surface. Upon irradiation by light ($\lambda > 420$ nm), both the clusters and their silica composites can generate singlet oxygen, demonstrating the oxygen permeability of silica. The smaller silica-cluster composites are potential candidates for photodynamic therapy and for other applications of singlet oxygen. The encapsulation is ineffective for neutral and anionic clusters. Electrostatic interaction between cationic clusters and the anionic, deprotonated silanol groups is proposed to drive the encapsulation.

Introduction

Singlet oxygen (denoted as $^1O_2$) is a nonpolluting oxidant that is available in abundance from air and light. Interest in the reaction chemistry of $^1O_2$ extends from the benchtop to the refinery to the clinic.[1] Singlet oxygen oxidation of alkenes is regioselective and stereoselective.[2] Product mixtures are sensitive to the steric and electronic features of the olefin.[3−10] Reaction outcomes can also be environmentally dictated, as in zeolite cavities.[11−13] The electrostatics of the cavity, and the conformational changes inside it, can be stereodirecting.

Singlet oxygen is also feasible for treating wastewater. Sulfide salts are water pollutants that result from food processing, tanning, natural gas purifying, and oil refining. Reactions with singlet oxygen transform sulfides to sulfates. Similarly, phenols contaminate wastewater from dye and paper manufacturing; they also result from petroleum refining. Phenol oxidation by $^1O_2$ has also been investigated for wastewater treatment.[14,15]

The term "photodynamic effect" refers to the action of oxygen and light on living cells and tissues. An example is the sterilization of blood plasma with the photosensitizer methylene blue. Frozen plasma donations have been treated this way by the Swiss and German Red Cross. Methylene blue is a nontoxic sensitizing dye. However, enzymatic reduction leads to a colorless product, and methylene blue loses its sensitizing effects.[16]

"Photodynamic therapy" (PDT) is the clinical use of light to attack tumors while sparing healthy tissue.[17−19] Practitioners recognize two variants:[20−22] Type I PDT is an electron-transfer process that forms ground-state

*Corresponding author.

(1) DeRosa, M. C.; Crutchley, R. J. *Coord. Chem. Rev.* **2002**, *233−234*, 351–371.
(2) Carey, F. A.; Sundberg, R. J. *Advanced Organic Chemistry Part B: Reactions and Synthesis*, 5th ed.; Springer: New York, 2007; pp 1117−1124.
(3) Orfanopoulos, M.; Grdina, M. B.; Stephenson, L. M. *J. Am. Chem. Soc.* **1979**, *101*, 275–276.
(4) Schulte-Elte, K. H.; Muller, B. L.; Rautenstrauch, V. *Helv. Chim. Acta* **1978**, *61*, 2777–2783.
(5) Schulte-Elte, K. H.; Rautenstrauch, V. *J. Am. Chem. Soc.* **1980**, *102*, 1738–1740.
(6) Clennan, E. L.; Chen, X.; Koola, J. J. *J. Am. Chem. Soc.* **1990**, *112*, 5193–5199.
(7) Adam, W.; Nestler, B. *J. Am. Chem. Soc.* **1992**, *114*, 6549–6550.
(8) Adam, W.; Nestler, B. *J. Am. Chem. Soc.* **1993**, *115*, 5041–5049.
(9) Stratakis, M.; Orfanopoulos, M.; Foote, C. S. *Tetrahedron Lett.* **1996**, *37*, 7159–7162.
(10) Brunker, H.-G.; Adam, W. *J. Am. Chem. Soc.* **1995**, *117*, 3976–3982.
(11) Li, X.; Ramamurthy, J. *J. Am. Chem. Soc.* **1996**, *118*, 10666–10667.
(12) Stratakis, M.; Rabalakos, C.; Mpourmpakis, G.; Froudakis, L. G. *J. Org. Chem.* **2003**, *68*, 2839–2843.
(13) Pace, A.; Clennan, E. L. *J. Am. Chem. Soc.* **2002**, *124*, 11236–11237.
(14) Nowakowska, M.; Kepczynski, M. *J. Photochem. Photobiol. A: Photochem.* **1998**, *116*, 251–256.
(15) Gerdes, R.; Bartels, O.; Schneider, G.; Wöhrle, D.; Schulz-Ekloff, G. *Polym. Adv. Technol.* **2001**, *12*, 152–160.
(16) Sharman, W. M.; Allen, G. M.; VanLier, J. E. *Drug Discovery Today* **1999**, *4*, 507–517.
(17) Castano, A. P.; Mroz, P.; Hamblin, M. R. *Nat. Rev. Cancer* **2006**, *6*, 535–545.
(18) Dolmans, D. E. J. G. J.; Fukumura, D.; Jain, R. K. *Nat. Rev. Cancer* **2003**, *3*, 380–387.
(19) Oleinick, N. L.; Morris, R. L.; Belichenko, I. *Photochem. Photobiol. Sci.* **2002**, *1*, 1–21.

 Published on Web 11/10/2010

reactive oxygen species (O_2^-, OH·, and H_2O_2, among others), whereas Type II PDT generates singlet oxygen. Energy transfer from a sensitizing dye to $^3O_2$ forms excited $^1O_2$. Sensitized oxygen is a mobile reagent that oxidizes amino acid residues, lipids, nucleic acids, and other biomolecules. The ensuing oxidative stress kills cells via apoptosis (programmed cell death) or necrosis (nonspecific cell death). Where cell death is concentrated, local inflammation can result. An immune-system response against malignant cells follows.

Developing photosensitizers for human cancer treatment draws continuing effort. A perfect PDT sensitizer has a fixed composition and uniform purity. It should be selective for tumor tissue and accumulate quickly therein. The photosensitizer should absorb at a wavelength of 600−900 nm, where human tissue is comparatively transparent. Sensitizers should be stable to light and physiological fluids; they should be nontoxic in darkness. After treatment, photosensitizers should clear the body rapidly and completely. No known photosensitizing drug is fully satisfactory.[23]

The most debilitating issue in PDT is toxicity. Various efforts have embedded sensitizers in drug delivery vehicles.[24] Oil dispersions (micelles), liposomes, low-density lipoproteins, polymeric micelles, and hydrophilic drug-polymer complexes have been used as carriers to deliver hydrophobic photodrugs that cannot be easily administered in saline solution.[25,26] These colloidal carriers accumulate passively in tumors by the enhanced permeability and retention effect.[27,28] Some successes have been achieved with oil-based drug carriers, including reduced drug loadings and improved tumor uptake.[29,30] However, the emulsifiers can induce allergic reactions in some patients.[31,32] Many liposomal carriers suffer from poor drug loadings and from self-aggregation of the drug when trapped. Liposomes are also prone to opsonization and capture by the reticuloendothelial system.[33] Sensitizers have been incorporated in pH-sensitive polymer micelles, but drug buildup in normal tissue and poor tumor regression have resulted.[34] Moreover, because these polymer-based drug carriers work on a controlled-release basis, post-treatment accumulation of the free drug in the skin and eyes is unavoidable. Side effects linger for weeks.[35]

Nanoparticles have been explored as delivery systems for photodrugs.[36,37] A hydrophilic three-component drug delivery system results from coating a zinc-phthalocyanine sensitizer and a transfer agent on gold nanoparticles.[38] The composite generates singlet oxygen with enhanced efficiency, compared to the free phthalocyanine. Similarly, excitation of the silicon phthalocyanine drug Pc4 was facilitated through FRET upon adsorption to CdSe quantum dots. Singlet oxygen was detected optically.[39] However, the cytotoxicity of cadmium-based quantum dots precludes their application in photodynamic therapy.[40−44]

Another potential drug carrier is nanosilica.[45,46] Silica is nontoxic and biocompatible. It is transparent to visible light, and it is inert to electron transfer and energy transfer. Silica particles are easily prepared under ambient conditions in the sol−gel process. Particle sizes are readily controlled.[47,48] Importantly, silica is porous to oxygen.[49−54] Because silica particles maintain their structures under harsh conditions, they can protect encapsulated drugs.[55,56] A further advantage is that silica surfaces are easily modified with functional groups that impart water solubility

(20) Szaciłowski, K.; Macyk, W.; Drzewieka-Matuszek, A.; Brindell, M.; Stochel, G. *Chem. Rev*. **2005**, *105*, 2647–2694.
(21) Dougherty, T. J. *Adv. Photochem*. **1992**, *17*, 275–311.
(22) Manda, G.; Nechifor, M. T.; Neagu, T.-M. *Curr. Chem. Biol*. **2009**, *3*, 342–366.
(23) Lovell, J. F.; Liu, T. W. B.; Chen, J.; Zheng, G. *Chem. Rev*. **2010**, *110*, 2839–2857.
(24) Damoiseau, X.; Schuitmaker, H. J.; Lagerberg, J. W. M.; Hoebeke, M. *J. Photochem. Photobiol., B: Biol*. **2001**, *60*, 50–60.
(25) Konan, Y. N.; Gruny, R.; Allemann, E. *J. Photochem. Photobiol., B: Biol*. **2002**, *66*, 89–106.
(26) Taillefer, J.; Jones, M.-C.; Brasseur, N.; Van Lier, J. E.; Leroux, J.-C. *J. Pharm. Sci*. **2000**, *89*, 52–62.
(27) Maeda, H.; Seymour, L. W.; Miyamoto, Y. *Bioconjugate Chem*. **1992**, *3*, 351–362.
(28) Iyer, A. K.; Khaled, G.; Fang, J.; Maeda, H. *Drug Discovery Today* **2006**, *11*, 812–818.
(29) Kongshaug, M.; Moan, J.; Cheng, L. S.; Garbo, G. M.; Kolboe, S.; Morgan, A. R.; Rimington, C. *Int. J. Biochem*. **1993**, *25*, 739–760.
(30) Woodburn, K.; Kessel, D. *J. Photochem. Photobiol., B: Biol*. **1994**, *22*, 197–201.
(31) Dye, D.; Watkins, J. *Br. Med. J*. **1980**, *280*, 1353.
(32) Michaud, L. B. *Ann. Pharmacother*. **1997**, *31*, 1402–1404.
(33) Isele, U.; Schieweck, K.; Kessler, R.; von Hoogevest, P.; Caparo, H.-G. *J. Pharm. Sci*. **1995**, *84*, 166–173.
(34) Taillefer, J.; Brasseur, N.; Van Lier, J. E.; Lenaerts, V.; Le Garrec, D.; Leroux, J. C. *J. Pharm. Pharmacol*. **2001**, *53*, 155–166.
(35) Dillon, J.; Kennedy, J. C.; Pottier, R. H.; Roberts, J. E. *Photochem. Photobiol*. **1988**, *48*, 235–238.
(36) Bechet, D.; Couleaud, P.; Frochot, C.; Viriot, M.-L.; Guillemin, F.; Barberi-Heyob, M. *Trends Biotechnol*. **2008**, *26*, 612–621.
(37) Delehanty, J. B.; Mattoussi, H.; Medintz, I. *Anal. Bioanal. Chem*. **2009**, *393*, 1091–1105.
(38) Hone, D. C.; Walker, P. I.; Evans-Gowing, R.; FitzGerald, S.; Beeby, A.; Chambrier, I.; Cook, M. J.; Russell, D. A. *Langmuir* **2002**, *18*, 2985–2987.
(39) Samia, A. C. S.; Chen, X.; Burda, C. *J. Am. Chem. Soc*. **2003**, *125*, 15736–15737.
(40) Derfus, A. M.; Chan, W. C. W.; Bhatia, S. N. *Nano Lett*. **2004**, *4*, 11–18.
(41) Hoshino, A.; Fujioka, K.; Oku, T.; Suga, M.; Sasaki, Y. F.; Ohta, T.; Yasuhara, M.; Suzuki, K.; Yamamoto, K. *Nano Lett*. **2004**, *4*, 2163–2169.
(42) Kirchner, C.; Liedl, T.; Kudera, S.; Pellegrino, T.; Javier, A. M.; Gaub, H. E.; Stolzle, S.; Fertig, N.; Parak, W. J. *Nano Lett*. **2005**, *5*, 331–338.
(43) Hardman, R. A. *Environ. Health Persp*. **2006**, *114*, 165–172.
(44) Cho, S. J.; Maysinger, D.; Jain, M.; Roder, B.; Hackbarth, S.; Winnik, F. M. *Langmuir* **2007**, *23*, 1974–1980.
(45) Montalti, M.; Prodi, L.; Zaccheroni, N.; Falini, G. *J. Am. Chem. Soc*. **2002**, *124*, 13540–13546.
(46) Roy, I.; Ohulchanskyy, T. Y.; Pudavar, H. E.; Bergey, E. J.; Oseroff, A. R.; Morgan, J.; Dougherty, T. J.; Prasad, P. N. *J. Am. Chem. Soc*. **2003**, *125*, 7860–7865.
(47) Brinker, C. J.; Scherer, G. W. *Sol−Gel Science: The Physics and Chemistry of Sol−Gel Processing*; Academic Press: San Diego, CA, 1990.
(48) Avnir, D.; Braun, S.; Lev, O.; Ottolenghi, O. *Chem. Mater*. **1994**, *6*, 1605–1614.
(49) Jorge, P. A. S.; Caldas, P.; Rosa, C. C.; Oliva, A. G.; Santos, J. L. *Sens. Actuators B* **2004**, *103*, 290–299.
(50) Zhang, P.; Guo, J.; Wang, Y.; Pang, W. *Mater. Lett*. **2002**, *53*, 400–405.
(51) Nooney, R. I.; Dhanasekaran, T.; Chen, Y.; Josephs, R.; Ostafin, A. E. *Adv. Mater*. **2002**, *14*, 529–532.
(52) Levin, P. P.; Costa, S. M. B.; Viera Ferreira, L. F.; Lopes, J. M.; Ramôa Ribeiro, F. *J. Phys. Chem. B* **1997**, *101*, 1355–1363.
(53) McEvoy, A. K.; McDonagh, C. M.; MacCraith, B. D. *Analyst* **1996**, *121*, 785–788.
(54) Samuel, J.; Ottolenghi, M.; Avnir, D. *J. Phys. Chem*. **1992**, *96*, 6398–6405.
(55) Weetal, H. H. *Biochim. Biophys. Acta* **1970**, *212*, 1–7.
(56) Jain, T. K.; Roy, I.; De, T. K.; Maitra, A. N. *J. Am. Chem. Soc*. **1998**, *120*, 11092–11095.

and tumor-cell selectivity.[57,58] Recent efforts have emplaced organic molecules in nanosilica. One method first links dye molecules to a silane coupling agent that is subsequently used in the hydrolysis of tetraethoxysilane in mixtures of water, aqueous ammonia, and ethanol.[59] Fluorescent silica nanoparticles with the dye molecules distributed in various ways have been successfully synthesized. An example is the incorporation of *meta*-tetra-(hydroxyphenyl)chlorine in nanosilica by this method.[60] Although singlet oxygen generation was observed, the average particle size was ~180 nm, which is far outside the size limit for kidney clearance (≤20 nm). Another encapsulation of organic dyes[46] and cadmium chalcogenide nanocrystals[61] in silica uses a micellar system. The photodrug 2-devinyl-2-(1-hexyloxyethyl)pyropheophorbide (HPPH) has been successfully incorporated in silica nanoparticles (~30 nm) in surfactant/1-butanol/water micelles.[46] Singlet oxygen generation was efficient, and irradiation caused destruction of tumor cells impregnated with the dye-doped silica nanoparticles. However, decreasing the particle size further is an ongoing challenge.

Hexanuclear clusters of molybdenum(II) and tungsten-(II) are powerful singlet oxygen generators.[62,63] Their photosensitization quantum yields exceed those of competing photodrugs, such as Pc4,[64] lutetium(III) texaphyrin,[65] and colloidal CdSe.[39] Their isostructural rhenium-(III) analogues[66−68] also luminesce through a spin-triplet state with quenching by oxygen.[69−74] These rhenium(III) clusters undergo ligand substitution reactions with σ-nucleophiles, typically organophosphines.[75−78] Trialkylphosphine-terminated rhenium(III) clusters survive heating, photolysis, and electrochemical oxidation. The cluster stereochemistry and core structure are maintained during ligand substitution.[79] Emission properties can be finely tuned by changing the axial ligands.[80,81] However, potential dark toxicity may come from the heavy-element composition of the cluster cores.

Here, we report the synthesis of hexanuclear cluster-doped silica nanoparticles based on the hydrolysis of tetraethylorthosilicate (TEOS) in a one-pot reaction system. The hexanuclear clusters used are rhenium(III) chalcogenide clusters with trialkylphosphine terminal ligands. Among these is the site-differentiated[82−84] cluster $[Re_6Se_8(Bu_3P)_5I]I$, which is described here for the first time. The size of the cluster-doped silica nanoparticles is within 10−15 nm, and the absorption and emission properties of the clusters were maintained in silica nanoparticles. Upon illumination, the clusters and their silica composites generate singlet oxygen.

Experimental Section

Operations involving trialkylphosphines were conducted with standard Schlenk techniques. Reagents were commercial and were used as received. Solvents were passed through an Mbraun solvent purification system before use. Nuclear magnetic resonance (NMR) spectra (^{1}H and ^{31}P{^{1}H}) were recorded on a Varian Model AS-400 spectrometer operating at 399.7 and 161.8 MHz, respectively. For ^{1}H NMR spectra, chemical shifts were determined relative to the solvent residual peaks. For ^{31}P{^{1}H} NMR spectra, chemicals shifts were determined relative to 85% $H_3PO_4(aq)$. Because of the small scale of the preparations, new compounds were not analyzed.

Morphology studies were performed on a JEOL Model 1200CX transmission electron microscopy (TEM) system, with the accelerating voltage being 80 kV. To prepare a TEM sample, a small amount of the powder was dispersed in ethanol under sonication, a drop of the dispersion was adsorbed on a carbon-supported copper grid, and the solvent was allowed to evaporate prior to measurement.

A Varian ultraviolet−visible-light−near-infrared (UV−vis−NIR) spectrophotometer (Model Cary 5G) and a Varian Eclipse fluorescence spectrophotometer were used for optical measurements. Solid cluster samples were dissolved in acetonitrile for absorption and emission spectra collection. Powders of the silica-cluster composites were suspended in hexanol or chloroform, and the upper clear solution was used for characterization.

Singlet oxygen generation was performed on a sun-simulating xenon lamp with a filtered light wavelength longer than 420 nm.

(57) Badley, R. D.; Warren, T. F.; McEnroe, F. J.; Assink, R. A. *Langmuir* **1990**, *6*, 792–801.
(58) Lal, M.; Levy, L.; Kim, K. S.; He, G. S.; Wang, X.; Min, Y. H.; Pakatchi, S.; Prasad, P. N. *Chem. Mater.* **2000**, *12*, 2632–2639.
(59) Blaaderen, A. V.; Vrij, A. *Langmuir* **1992**, *8*, 2921–2931.
(60) Yan, F.; Kopelman, R. *Photochem. Photobiol.* **2003**, *78*, 587–591.
(61) Graf, C.; Dembski, S.; Hofmann, A.; Ruehl, E. *Langmuir* **2006**, *22*, 5604–5610.
(62) Jackson, J. A.; Turró, C.; Newsham, M. D.; Nocera, D. G. *J. Phys. Chem.* **1990**, *94*, 4500–4507.
(63) Jackson, J. A.; Newsham, M. D.; Worsham, C.; Nocera, D. G. *Chem. Mater.* **1996**, *8*, 558–564.
(64) He, J.; Larkin, H. E.; Li, Y.; Rither, B. D.; Zaidi, S. I. A.; Rodgers, M. A. J.; Hasan, M.; Kenney, M. E.; Oleinick, N. L. *Photochem. Photobiol.* **1997**, *65*, 581–586.
(65) Grossweiner, L. I.; Bilgin, M. D.; Berdusis, P.; Mody, T. D. *Photochem. Photobiol.* **1999**, *70*, 138–145.
(66) Long, J. R.; McCarty, L. S.; Holm, R. H. *J. Am. Chem. Soc.* **1996**, *118*, 4603–4616.
(67) Gabriel, J.-C. P.; Boubekeur, K.; Uriel, S.; Batail, P. *Chem. Rev.* **2001**, *101*, 2037–2066.
(68) Gray, T. G. *Coord. Chem. Rev.* **2003**, *243*, 213–235.
(69) Gray, T. G.; Rudzinski, C. M.; Nocera, D. G.; Holm, R. H. *Inorg. Chem.* **1999**, *38*, 5932–5933.
(70) Yoshimura, T.; Ishizaka, S.; Umakoshi, K.; Sasaki, Y.; Kim, H.-B.; Kitamura, N. *Chem. Lett.* **1999**, 697–698.
(71) Yoshimura, T.; Umakoshi, K.; Sasaki, Y.; Ishizaka, S.; Kim, H.-B.; Kitamura, N. *Inorg. Chem.* **2000**, *39*, 1765–1772.
(72) Chen, Z.-N.; Yoshimura, T.; Abe, M.; Tsuge, K.; Sasaki, Y.; Ishizaka, S.; Kim, H.-B.; Kitamura, N. *Chem.—Eur. J.* **2001**, *7*, 4447–4455.
(73) Kahnt, A.; Heiniger, L.-P.; Liu, S.-X.; Tu, X.; Zheng, Z.; Hauser, A.; Decurtins, S.; Guldi, D. M. *ChemPhysChem* **2010**, *11*, 651–658.
(74) Yoshimura, T.; Suo, C.; Tsuge, K.; Ishizaka, S.; Nozaki, K.; Sasaki, Y.; Kitamura, N.; Shinohara, A. *Inorg. Chem.* **2010**, *49*, 531–540.
(75) Willer, M. W.; Long, J. R.; McLauchlan, C. C.; Holm, R. H. *Inorg. Chem.* **1998**, *37*, 328–333.
(76) Zheng, Z.; Long, J. R.; Holm, R. H. *J. Am. Chem. Soc.* **1997**, *119*, 2163–2171.
(77) Shestopalov, M. A.; Mironov, Y. V.; Brylev, K. A.; Kozlova, S. G.; Fedorov, V. E.; Spies, H.; Pietzsch, H.-J. H.; Stephan, H.; Geipel, G.; Bernhard, G. *J. Am. Chem. Soc.* **2007**, *129*, 3714–3721.
(78) Perruchas, S.; Avarvari, N.; Rondeau, D.; Levillain, E.; Batail, P. *Inorg. Chem.* **2005**, *44*, 3459–3465.
(79) Zheng, Z.; Gray, T. G.; Holm, R. H. *Inorg. Chem.* **1999**, *38*, 4888–4895.
(80) Gray, T. G.; Rudzinski, C. M.; Meyer, E. E.; Holm, R. H.; Nocera, D. G. *J. Am. Chem. Soc.* **2003**, *125*, 4755–4770.
(81) Yoshimura, T.; Umakoshi, K.; Sasaki, Y.; Sykes, A. G. *Inorg. Chem.* **1999**, *38*, 5557–5564.
(82) Holm, R. H.; Ciurli, S.; Weigel, J. A. *Prog. Inorg. Chem.* **1990**, *38*, 1–74.
(83) Gray, T. G.; Holm, R. H. *Inorg. Chem.* **2002**, *41*, 4211–4216.
(84) Selby, H. D.; Roland, B. K.; Zheng, Z. *Acc. Chem. Res.* **2003**, *36*, 933–944.

Syntheses. The clusters $[Re_6Se_8(Et_3P)_5I]I$ and $[Re_6S_8(Et_3P)_5Br]Br$ were prepared according to published procedures.[75,76]

[Re$_6$Se$_8$(Bu$_3$P)$_5$I]I. In a 100-mL round-bottom flask, $(Bu_4N)_3[Re_6S_8I_6]$ (500 mg, 0.15 mmol) was dissolved in *N,N*-dimethylformamide and degassed. Tributylphosphine (0.31 mL, 1.24 mmol, 8 equiv) was added and refluxed 24 h under argon. The solvent was removed by cold trap and the resulting deep red residue was washed several times with diethyl ether (100 mL total) and dissolved in a small amount of methylene chloride. Silica-gel column chromatography was conducted. The product was recovered with 1:1 chloromethane:acetonitrile. ^{31}P NMR: δ −38.0 (4), −39.8 (1) ppm; 79% yield.

[Re$_6$S$_8$(Bu$_3$P)$_5$Br]Br. $(Bu_4N)_4Re_6S_8Br_6 \cdot H_2O$ (200 mg, 0.07 mmol) was dissolved in 10 mL of dimethylformamide (DMF) and degassed. Argon-saturated tributylphosphine (0.46 mL, 1.86 mmol) was added to the solution. The resulting mixture was refluxed under argon for 48 h. The solvent was removed in vacuo, and the oily residue was triturated using ether to give an orange-red powder. The powder was dissolved in a minimal volume of methylene chloride, and the solution was subjected to chromatography on a silica gel column. Elution with methylene chloride afforded an orange fraction, tentatively identified as *cis*-$[Re_6S_8(Bu_3P)_4Br_2]$. A second fraction eluted with acetonitrile was the desired product. Solid products were not collected, and the acetonitrile solution was used for further experiments.

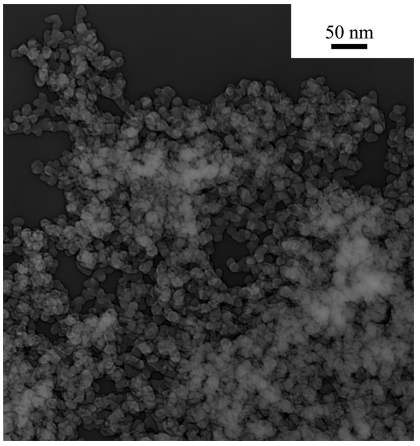

Figure 1. TEM images for the silica−$[Re_6Se_8(Bu_3P)_5I]I$ composites, showing that the diameter of the nanoparticles is within the range of 10−20 nm.

Synthesis of Silica-Cluster Composites. Typically, 3.7 mL of tetraethylorthosilicate (TEOS) was mixed with 3 mL of distilled water and 0.8 mL aqueous ammonia (28−30%), and then stirred to form a gel (~15 min). To the gel, 1 mL of acetonitrile solution of the cluster was added under rapid stirring. The mixture was then stirred for another 2 h. The products were filtered to give a yellow powder, which was washed repeatedly using acetonitrile until the filtrate was colorless, and dried in the air.

Singlet Oxygen Generation and Detection. The singlet oxygen indicator 2,3-diphenyl-*p*-dioxene was prepared following a published procedure.[85] To a quartz emission cuvette was added a deuterated acetone solution of the cluster or silica-cluster composite. The compound 2,3-diphenyl-*p*-dioxene was dissolved in the solution (typically 0.2 M). The mixture was oxygen-saturated by bubbling compressed oxygen into the solution for 20 min. The cuvette was then exposed to the irradiation source with light that had a wavelength longer than 420 nm. An aliquot of the solution was withdrawn at different irradiation intervals and added to an NMR tube. ^{1}H NMR data were then collected.

Results and Discussion

All four positively charged clusters were incorporated within silica successfully. Similar experiments conducted on negatively charged ($[Re_6S_8Br_6]^{4-}$) or charge-neutral clusters (*cis*- and *trans*-$[Re_6S_8(Et_3P)_4Br_2]$) yielded white powders without detectable absorption or emission of the clusters. Usually, a strong interaction is required when incorporating fluorescent dyes in silica nanoparticles. Here, we propose that the encapsulation was made possible by an electrostatic interaction between cationic clusters and the anionic, deprotonated silanol groups generated in the base-catalyzed hydrolysis process.

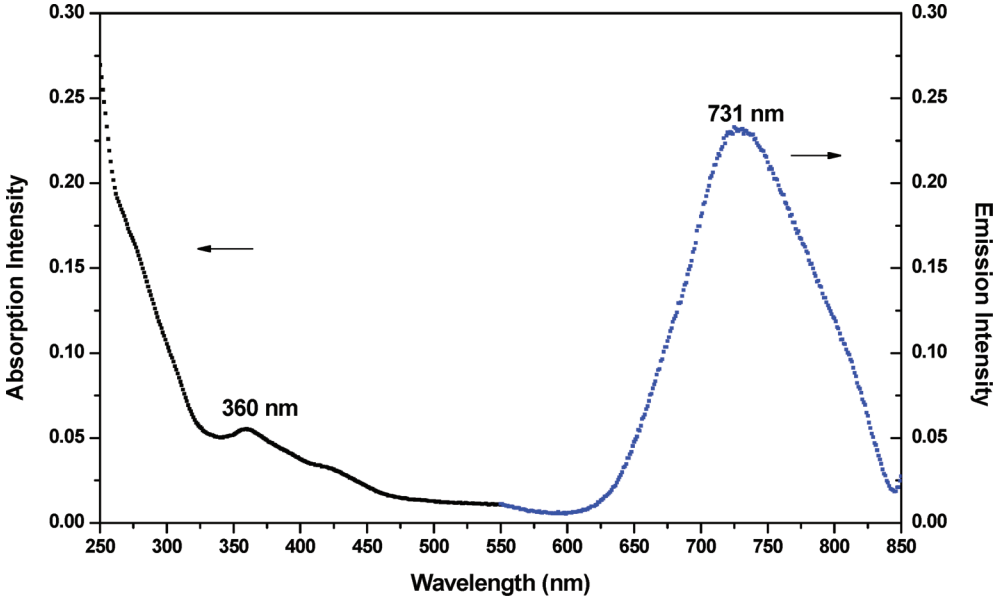

Figure 2. Absorption and emission of silica−$[Re_6Se_8(Bu_3P)_5I]I$ composite collected in hexanol, in air. The excitation wavelength used is 430 nm, and the slit width is 5 nm.

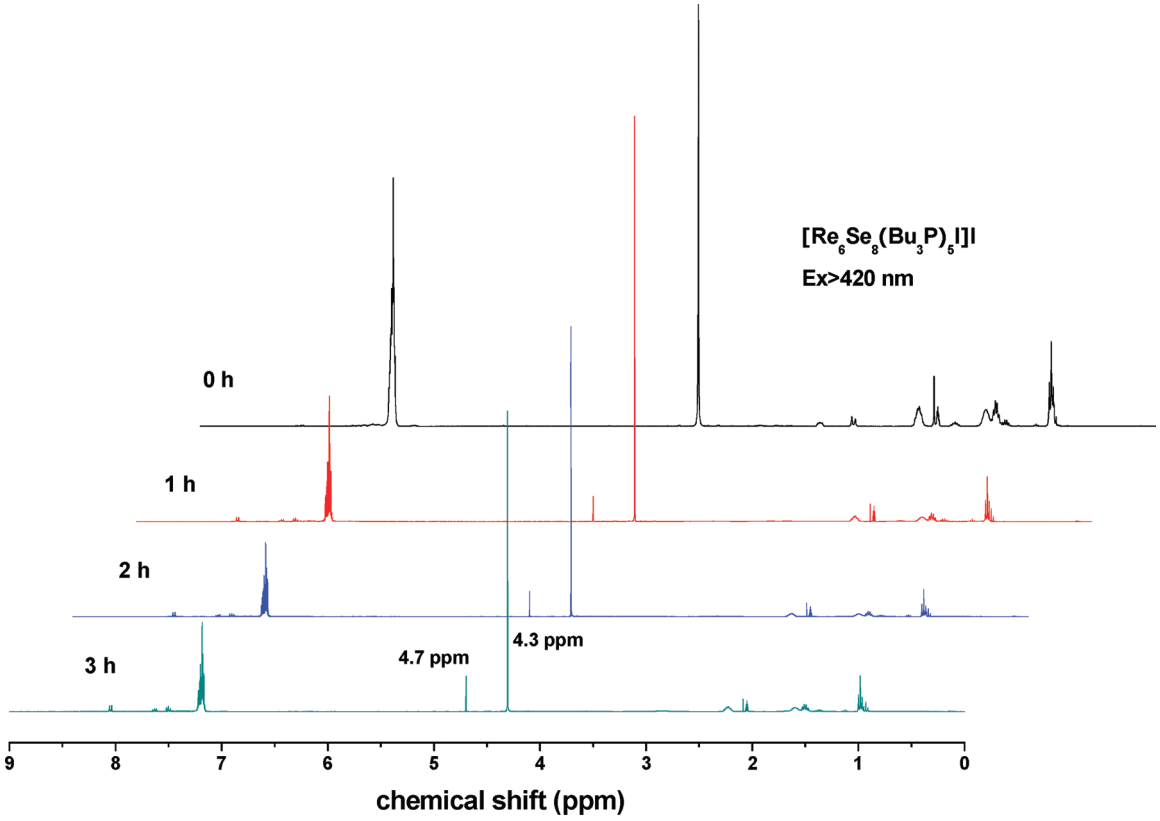

Figure 3. ^{1}H NMR spectra for oxygen saturated deuterated acetone solution of $[Re_6Se_8(Bu_3P)_5I]I$ mixed with the singlet oxygen indicator, 2,3-diphenyl-*p*-dioxene, collected at 1 h, 2 and 3 h irradiation intervals. The resonances of butyl groups and solvent appear within 0.9−2.5 ppm.

Morphology Study of the Silica−Cluster Composite. Figure 1 shows a typical TEM image for the silica−$[Re_6Se_8(Bu_3P)_5I]I$ composite prepared with 1 mL of an acetonitrile solution of clusters. Surface interaction between the small nanoparticles results in the aggregation. Control experiments were conducted by changing the volume used to dissolve the clusters in the preparation step. For acetonitrile volumes below 5 mL, nanoparticles with diameters of 10−20 nm can be readily observed. When the volume of acetonitrile reaches 10 mL, large particles with diameters of ∼200 nm are found (see the Supporting Information). With a constant volume of acetonitrile, no morphology difference was observed when changing the amount or type of the clusters.

Optical Properties. Incorporation in silica preserved the absorption and emission profiles of entrapped clusters. Optical measurements are possible because the refractive indices of 1-hexanol and chloroform are similar to that of silica (∼1.5). Suspensions of silica composites in these solvents are optically transparent.[86,87]

Figure 2 shows absorption and emission spectra of the silica−$[Re_6Se_8(Bu_3P)_5I]I$ composite collected in hexanol. These are similar to spectra of the free cluster collected in acetonitrile. Optical spectra of the composites of the other three clusters—silica−$[Re_6Se_8(PEt_3)_5I]I$, silica−$[Re_6S_8(PEt_3)_5Br]Br$, and silica−$[Re_6S_8(Bu_3P)_5Br]Br$—all resemble the spectra of their corresponding clusters, which are shown in the Supporting Information. A rigidochromic blue-shift of 6 nm was observed when comparing the emission spectra of the degassed chloroform solutions of $[Re_6Se_8(Bu_3P)_5I]I$ and silica−$[Re_6Se_8(Bu_3P)_5I]I$, and a 10-nm shift was observed for $[Re_6Se_8(Et_3P)_5I]I$ and silica−$[Re_6Se_8(Et_3P)_5I]I$, indicating that the clusters reside in the silica framework. Optical properties of the embedded clusters are unchanged upon standing in air indefinitely (months). Furthermore, the nanocomposites that contain clusters are luminescent in air at room temperature. In contrast, unembedded clusters do not visibly emit in air.

Singlet Oxygen Generation. Emission of both degassed chloroform solutions of the clusters and their silica−cluster composites was measured. Emission was quenched when the solutions were exposed to air. This observation indicates (i) an interaction between the emitting, triplet-state cluster and triplet oxygen, and (ii) that oxygen permeates the silica network.

The organic compound 2,3-diphenyl-*para*-dioxene (**1**)[85] is well-characterized as a singlet oxygen trap.[88,89] Its oxidation by $^1O_2$ in nonaqueous media yields ethylene glycol dibenzoate (**2**):

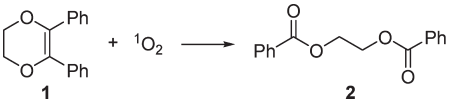

1 **2** (1)

The formation of **2** is easily discerned using ^{1}H NMR spectrometry. This reaction has been used previously

(85) Summerbell, R. K.; Berger, D. R. *J. Am. Chem. Soc.* **1959**, *81*, 633–639.
(86) van Helden, A. K.; Jansen, J. W.; Vrij, A. *J. Colloid Interface Sci.* **1981**, *81*, 354–368.
(87) Philipse, A. P.; Vrij, A. *J. Colloid Interface Sci.* **1989**, *128*, 121–136.
(88) Paczkowski, J.; Neckers, D. C. *ACS Symp. Ser.* **1985**, *278*, 222–242.
(89) Blossey, E. C.; Neckers, D. C.; Theyer, A. L.; Schaap, A. P. *J. Am. Chem. Soc.* **1973**, *95*, 5820–5823.

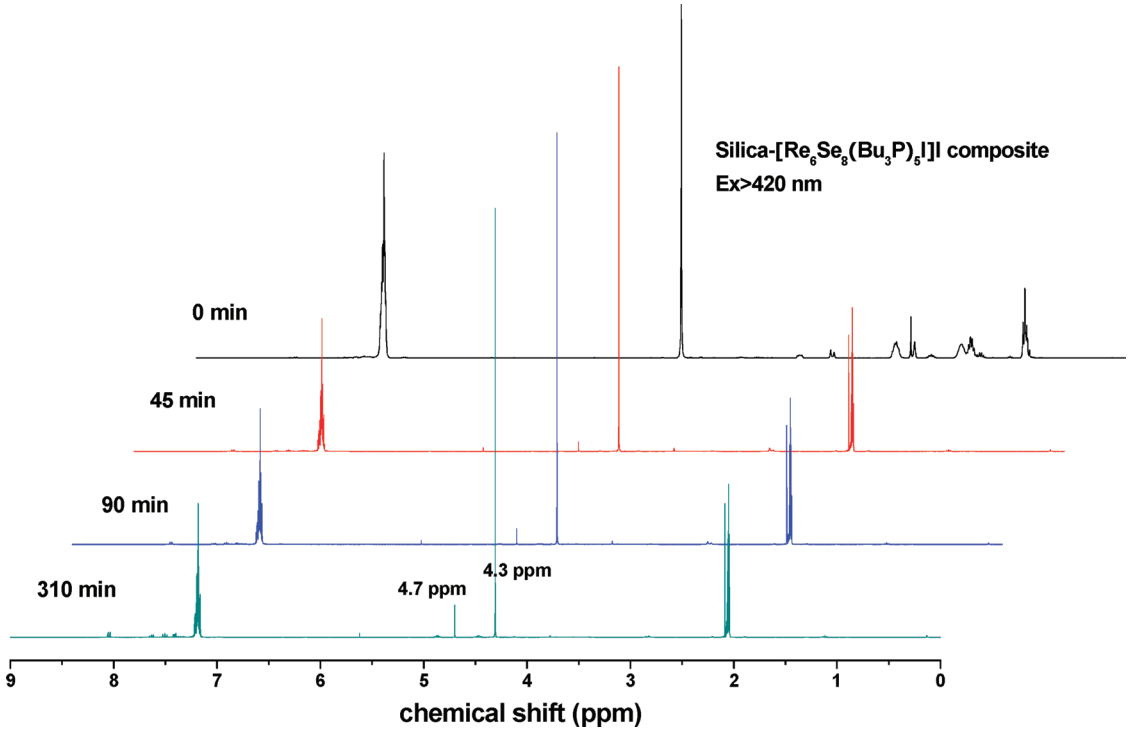

Figure 4. ^{1}H NMR spectra for oxygen-saturated deuterated acetone suspension of silica−$[Re_6Se_8(Bu_3P)_5I]I$ mixed with the singlet oxygen indicator, 2,3-diphenyl-*p*-dioxene, collected at irradiation intervals of 45, 90, and 310 min. $[Re_6Se_8(Bu_3P)_5I]I$ solution was used as the 0 min reference, showing the tributyl groups' resonance within 0.9−2.5 ppm.

to demonstrate oxygen sensitization by molybdenum(II) and tungsten(II) halide clusters.[62]

Figure 3 depicts ^{1}H NMR spectra of an acetone solution of **2** and $[Re_6Se_8(PBu_3)_5I]I$ collected after 1, 2, and 3 h of irradiation. The resonance at 4.3 ppm of the methylene protons of **1** shift to 4.7 ppm for **2**. The phenyl ring proton resonance at 7.2 ppm in **1** is split and shifts downfield in **2**. At longer irradiation times, the relative intensity (I(4.7 ppm)/I(4.3 ppm)) increases, as seen from peak integration. Furthermore, the splitting and downfield shift of the 7.2-ppm peak becomes more obvious. These observations indicate the efficient generation of singlet oxygen. Analogous experiments for the other three clusters yielded similar results, and NMR spectra appear in the Supporting Information. Control experiments found unreacted **1** in the absence of oxygen or irradiation.

Silica−cluster composites deposited on the bottom of the cuvette when suspended in deuterated acetone. For these, light was focused on the solid layer, and clear solutions were withdrawn for NMR measurement. ^{1}H NMR spectra appear in Figure 4. Resonances arising from the tributyl groups (0.9−2.5 ppm) were not seen in the solution that was withdrawn from the silica−$[Re_6Se_8(Bu_3P)_5I]I$ suspension (only solvent peaks are seen). This observation indicates that all the clusters are embedded in the silica framework and are not removed by the solvent. The intensity of the peak at 4.7 ppm increases when increasing the irradiation time, and the splitting and downfield shift of the peak at 7.2 ppm become more obvious, indicating that singlet oxygen can still be generated by the silica−cluster composites, and that oxygen permeates the silica framework.

Conclusions

Photoactive rhenium(III) chalcogenide clusters have been embedded in nanosilica, with control of the nanoparticle diameter. The immobilized clusters are lipophilic and cationic, with pendant trialkylphosphine ligands. Among them are the new species $[Re_6S_8(Bu_3P)_5Br]Br$ and $[Re_6Se_8(Bu_3P)_5I]I$. These complexes are unusual, site-differentiated Re_6 clusters prepared in high yields as the primary products of their syntheses. The new clusters emit red phosphorescence.

Clusters encased in silica retain triplet-state photoproperties. Room-temperature emission maxima are slightly blue-shifted, which is an expected outcome of trapping within a rigid matrix. Emission of the free clusters is quenched upon exposure to oxygen. Both the free clusters and their silica nanocomposites photo-oxidize 2,3-diphenyl-*para*-dioxene (**1**), indicating the formation of singlet oxygen. The sensitizing capabilities of rhenium(III) clusters and their nanocomposites are receiving further study.

Acknowledgment. The authors thank the donors of the Petroleum Research Fund, administered by the American Chemical Society (Grant 42312-G3 to T.G.G.), and the Alfred P. Sloan Foundation for support.

Supporting Information Available: Absorption and emission spectra of clusters and nanocomposites, NMR spectra, and TEM images. This information is available free of charge via the Internet at http://pubs.acs.org.